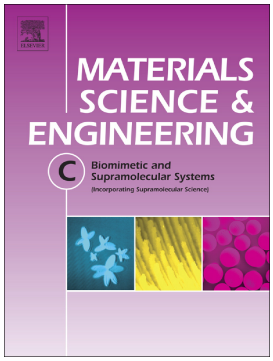

Sensitive impedimetric DNA biosensor based on (Nb,V) codoped TiO2 for breast cancer susceptible gene detection

Yu Wang, Xianwei Huang, He Li, Linlang Guo

PII: S0928-4931(16)30997-3
DOI: doi: 10.1016/j.msec.2017.03.260
Reference: MSC 7772

To appear in: *Materials Science & Engineering C*

Received date: 28 August 2016
Revised date: 27 December 2016

Please cite this article as: Yu Wang, Xianwei Huang, He Li, Linlang Guo , Sensitive impedimetric DNA biosensor based on (Nb,V) codoped TiO2 for breast cancer susceptible gene detection. The address for the corresponding author was captured as affiliation for all authors. Please check if appropriate. Msc(2017), doi: 10.1016/j.msec.2017.03.260

Sensitive impedimetric DNA biosensor based on (Nb,V) codoped TiO_2 for breast cancer susceptible gene detection

Yu Wang[1], Xianwei Huang[2], He Li[2], Linlang Guo[1,*]

[1]Department of Pathology, Zhujiang Hospital, Southern Medical University, Guangzhou 510282, China

[2]School of Chemistry and Environment, South China Normal University, Guangzhou 510006, China

*Author for correspondence:

Tel.: +86-20-62783359

zhujianghp@163.com

Abstract

In this paper, a novel (Nb,V) codoped TiO_2 (NVTO) nanoparticle was synthesized, and a novel electrochemical DNA biosensor based on NVTO was first developed for detection of breast cancer susceptible gene detection. The proposed DNA biosensors were fabricated by immobilization of the probe DNA on a nanoporous CHIT-NVTO thin film deposited on an ITO-coated glass plate. The prepared NVTO ccomposite film was characterized by XRD, SEM and FTIR. The results indicated that the synergistic effect of CHIT-NVTO nanocomposite can increase the electroactive surface area and the loading amounts of ssDNA. These can amplify the electrochemical signal resulting in increasing the sensitivity of the proposed biosensor. The proposed biosensor exhibited high sensitivity, wide linear range of 1.0×10^{-15} M ~ 1.0×10^{-6} M (r=0.9973) and a low detection limit of 1.09×10^{-16} M (S/N=3). The NVTO based biosensor opens a different perspective for susceptible gene detection and early diagnosis of breast cancer.

Key words: DNA biosensor; breast cancer susceptible gene; (Nb,V) codoped TiO_2

* Corresponding authors
Tel.: +86-20-62783359, zhujianghp@163.com

1. Introduction

Breast cancer which causes a worldwide public health concern is the second most common type of cancer and the second-leading cause of cancer death in women. BRCA1, a breast cancer susceptibility gene, is known as a kind of anti-oncogene and one of the most important breast cancer susceptibility gene [1,2,3]. BRCA1 mutation is closely associated with the occurrence of the family breast and ovary cancer. About 40%-50% of hereditary breast cancers are caused by BRCA1 mutation, however 80% patients whose BRCA1 have mutations in high incidence of family both breast and ovarian cancer [4]. Hence, the detection of BRCA1 offers an opportunity to characterize the function of genetic features in breast and ovarian cancer as well as to screen breast or ovarian cancer patients for the presence of germ line mutations [5].

Apparently, the discovery of BRCA1 mutation in patients can greatly affect the prediction of breast cancer risk and help the doctor and patient to take the appropriate steps for treatments. In recent years, many techniques such as single-strand conformation polymorphisms assay and DNA sequencing have been utilized for the screening of BRCA1 mutations [6,7]. These methods are well-proven and widely accepted; however, it is time-consuming, low sensitivity and high cost. Thus, low-cost, highly sensitive and highly selective detection methods are significant for rapid detection of BRCA1 mutations. In recent years, electrochemical DNA biosensors have received much attention due to the advantage of high sensitivity, rapid response, simplicity and high selectivity [8,9,10,11]. The electrochemical biosensor provides a simple, accurate and rapid platform for the early detection of breast carcinoma.

In recent years, a number of metal oxide nanoparticles such as CeO_2 [12], Fe_3O_4 [13], V_2O_5 [14], ZrO_2 [15], TiO_2 [16] have been utilized to immobilize carriers of DNA probe for electrochemical DNA biosensor due to their unique properties: large surface-to-volume ratio, high surface reaction activity, high catalytic efficiency, strong adsorption ability, electrical properties and excellent biocompatibility [17]. Metal oxide nanoparticles are playing an important role in the fabrication of electrochemical biosensor for the diagnosis of the infectious diseases. However, the electrochemical activities of these metal oxides applied in biosensors need to be improved further.

Chitosan (CHIT) is known as an interesting material with both strong inter- and intra-molecular hydrogen bonding interactions due to its hydroxyl and amino groups. It is one of the most widely used biopolymers for biosensor due to its nontoxic nature, excellent film forming ability, high permeability, and cost-effectiveness [18,19]. It is also a relatively stable electroactive biomaterial with excellent biocompatible property, which is conducive to immobilization of biomolecules over its surface [20]. Thus, CHIT was used to immobilize the biomolecule in this work.

Furthermore, doping metal oxide nanoparticles with a small amount of donor-type ions can improve its properties, such as electronic conductivity and ionic conductivity, compared with the prestine metal oxide[21,22]. In this study, a novel (Nb,V) codoped TiO_2 (NVTO) nanoparticles was first synthesized and successfully used in electrochemical DNA biosensors. DNA biosensors were then fabricated by immobilization of the probe DNA on a nanoporous CHIT-NVTO thin film deposited on an ITO-coated glass plate. The fabrication, characterization and analytical

performance of the proposed DNA biosensor based on CHIT-NVTO are described below.

2. Experimental

2.1 Materials

Ammonium niobate(V)oxalate hydrate, and tetrabutyl titanate were purchased from Sigma-Aldrich, USA; Chitosan(CHIT) were acquired from Amresco, USA. Ammonium metavanadate, TE hybridization buffer solution (10mM Tris-HCl, 1.0mM EDTA, pH=8.0), nitric acid, citric acid, ammonium hydroxide, sodium dihydrogen phosphate and sodium hydrogen phosphate were obtained from Aladdin, China.

The 26-base oligonucleotides probe (probe ssDNA), target complementary sequence DNA (target ssDNA), one-base mismatched ssDNA and two-base mismatched ssDNA sequence DNA related to BRCA1 gene were synthesized by Shanghai Invitrogen Trading Co., Ltd (China). These base sequences were shown in Table 1. Deionized water from the purification system has been utilized for preparation of the desired aqueous solutions.

Table 1 Oligonucleotide sequences used in this study.

Oligonucleotide	Sequence
Probe DNA (ssDNA)	5’-ATGTATGAATTATAATCAAAGAAACC-3’
Complementary target DNA (cDNA)	5’-GGTTTCTTTGATTATAATTCATACAT-3’
One-base mismatch DNA (OBM1)	5’-GGTTTCTTAGATTATAATTCATACAT-3’
One-base mismatch DNA (OBM2)	5’-GGTTTCTTTGATTATGATTCATACAT-3’
Two-base mismatch DNA (TBM1)	5’-GGTTTCTTAGATTATAAGTCATACAT-3’
Two-base mismatch DNA (TBM2)	5’-GGTTGCTTTGATTATGATTCATACAT-3’
noncomplementary DNA sequence(ncDNA)	5’-CTTCTGGTAGTCGGAGCTGATGGCG-3’

2.2 Preparation of (Nb,V) codoped TiO_2 (NVTO) nanoparticles

The preparation method of NVTO nanoparticles was according to our previously reported method with some modifications[23]. In detail, 6.0 g of citric acid ($C_6H_8O_7$) were dissolved in 200 mL of deionized water by heating and stirring at 80℃. 5mL of concentrated nitric acid solution were added after the citric acid completely dissolved. 3.5 mL of tetrabutyl titanate solution was then added into the above solution, with constant stirring for 2 h at 80°C~100 °C, to obtain clear and transparent solution. The pH value was adjust to 7.0 through dropwise adding ammonium hydroxide (NH_4OH) with stirring for 1~2h at 80~100 °C prior to dissolving 1.510 g of ammonium niobate (V) oxalate hydrate and 0.5850 g ammonium metavanadate in the solution. A swollen claybank sample was obtained by placing the solution into an oven at 200°C ~250°C, and then was sintered at 650 °C for 5 h to obtain nanoparticles of NVTO.

2.3 Preparation of the CHIT-NVTO/ITO nanocomposite electrodes

0.5% CHIT solution was prepared by dissolving 10 mg CHIT in 2.0 mL of acetate buffer (0.05 M, pH 4.2) solution. 2 mg of NVTO was dispersed in the CHIT solution by ultrasonication for more than 1h. 10 μL of the CHIT-NVTO solution was then transferred onto ITO surface and allowed to dry at room temperature. The CHIT-NVTO nanocomposite film was then washed with deionized water to remove any unbound particles.

2.4 DNA probe immobilization and hybridization

DNA solutions are prepared in TE buffer (10 mM Tris-HCl, 1.0 mM EDTA, pH=8.0). 10μL of freshly-prepared probe DNA solution (1.0×10^{-6} M) was spread onto

the CHIT-NVTO/ITO electrode and was air-dried at room temperature for 1 h to obtain a probe-modified electrode.

Hybridization reaction was conducted by pipetting 10 μL of hybridization buffer solution (0.1 M NaCl, 10mM Tris-HCl, 1.0mM EDTA) containing the target DNA of different concentration onto the surface of CHIT-NVTO electrode. This droplet was kept at 45°C for 1h. The electrode was washed with phosphate buffer (pH 7.0) to remove the unhybridized DNA.

2.5 Characterization

The characterization of the NVTO nanoparticles was determined by DSC/DTA-TG (STA449C，NETZSCH), X-ray diffraction (XRD, D8 ADVANCE, Bruker AXS), Fourier transform infrared spectroscopy (FTIR, Prestige-21, SHI-MADZU) and transmission electron microscopy (TEM，JEM-2100HR，JEOL). The surface morphologies of the electrodes were investigated using scanning electron microscopy (SEM, JSM-6330F, JEOL). Electrochemical analysis was conducted on an Autolab Potentiostat/Galvanostat (PGSTAT-30, Eco Chemie, Netherlands) using a three-electrode system with ITO as the working electrode, platinum (Pt) as the auxiliary electrode, and Ag/AgCl as the reference electrode in a phosphate buffer saline (PBS) solution (50 mM, pH 7.0, 0.9% NaCl) containing 1mM $[Fe(CN)_6]^{3-/4-}$ as the redox probe.

3. Results and discussion

3.1 Characterization of NVTO nanoparticles

The precursor of NVTO nanoparticles was investigated by DSC/DTA-TG from

room temperature to 800℃, and the result as shown in Figure 1A. It can be concluded that 500-650℃ is the process of forming and phase transformation of NVTO nanoparticles, so we choose 650℃ was the appropriate temperature of sample preparation. Figure 1B shows the XRD pattern of NVTO nanoparticles. All the XRD peaks were similar to the XRD peaks of rutile titanium dioxide, which indicates Nb and V was doped successfully without changing the crystallographic structure. Moreover, Nb, V and Ti element can be found in Figure S1. These data showed that the NVTO nanoparticle was synthesized sucessfully. The FTIR spectra of NVTO nanoparticles exhibited a sharp, intense peak at 518 cm^{-1}, which may be attributed to the stretching vibration bonding of Ti-O (Figure 1C). The TEM image of NVTO/ITO exhibits granular morphology with an average grain size of about 50 nm(Figure 1D).

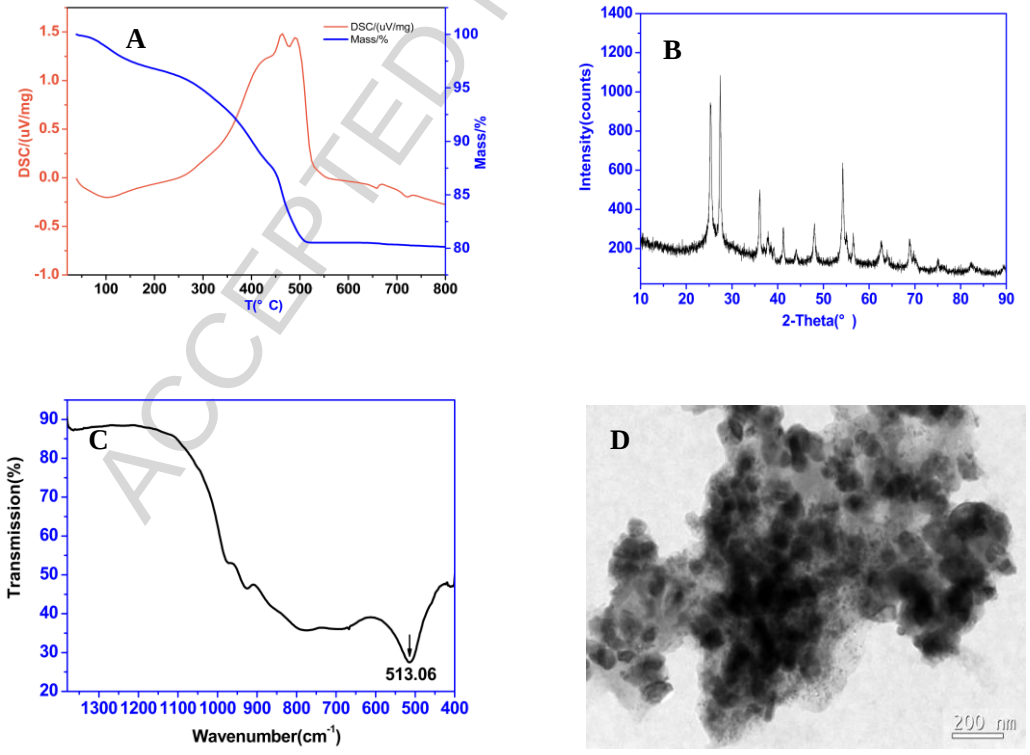

Figure 1 (A) Thermal Analysis of $Nb_{0.25}V_{0.25}Ti_{0.5}O_2$ nanoparticles, (B) X-ray diffraction pattern of $Nb_{0.25}V_{0.25}Ti_{0.5}O_2$ nanoparticles, (C) FTIR spectra of $Nb_{0.25}V_{0.25}Ti_{0.5}O_2$ nanoparticles, (D)

TEM of $Nb_{0.25}V_{0.25}Ti_{0.5}O_2$ nanoparticles

3.2 Surface morphology studies

The SEM image of CHIT/ITO showed that the thin film of CHIT spread evenly on the surface of ITO electrode (Figure 2A). The morphology of the CHIT-NTO/ITO electrode was showed in Figure 2B, it demonstrated that NVTO nanoparticles were regularly dispersed in the CHIT film and strongly adhered onto the substrate with porous network film, which might be attributed to electrostatic interactions between the cationic CHIT and postive charge on the surface of NVTO nanoparticles. The porous network of the CHIT-NVTO film resulted in increasing effective surface area of the substrate electrode to load large amounts of DNA, and also prevent the DNA molecules from leaching. These were conducive to response signal amplification of the resulted biosensor. After the immobilization of probe DNA, the surface roughness of morphology of ssDNA/ CHIT-NVTO/ITO (Figure 2C) indicated that the DNA probe had been firmly immobilized onto electrode surface by electrostatic interactions and covalent interactions between CHIT and probe DNA. Moreover, when DNA was entrapped in the porous network film, aggregates of the DNA molecules exhibited island-like structures that might accelerate specific reaction between substrate and DNA, resulting in enhanced amperometric response of the biosensor [24]. The surface morphology of ssDNA/CHIT-NVTO/ITO bioelectrode (Figure 2D) was found to be changed after hybridization with target DNA and indicated the hybridization was successful.

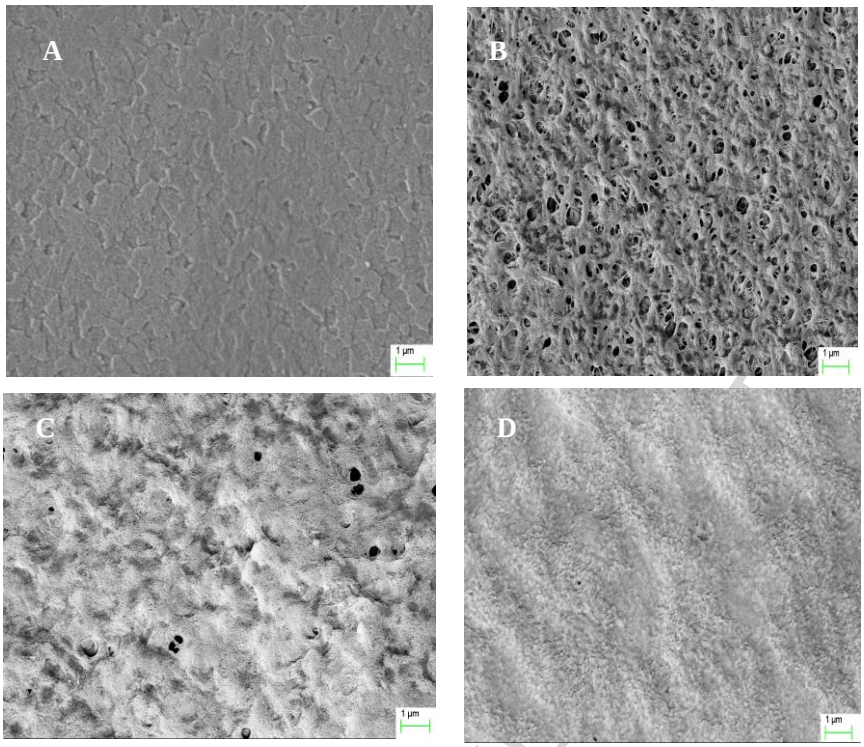

Figure 2 SEM images of the electrodes: (A) CHIT/ITO electrode, (B) CHIT-NVTO/ITO, (C) ssDNA/ CHIT-NVTO/ITO, (D) cDNA/ CHIT-NVTO/ITO

3.3 Electrochemical studies

Figure 3 (A) illustrated the differential pulse voltammograms (DPV) of various ITO-modified electrodes immersed in PBS in the potential range from -0.4 to 0.8V. The current for the CHIT/ITO electrode (curve b) increased drastically as compared to the current for ITO electrode (curve a), which might be due to the acceptance of electrons from the negatively-charged ferricyanide species in the PBS by cationic CHIT, resulting in increasing redox current. The significant increase in current response for the CHIT-NVTO/ITO electrode (curve c) suggested that the presence of NVTO nanoparticles increased electroactive surface area and therefore was benefit to electron transfer. The NVTO nanoparticle was conducive to electron transfer between redox probes in solution and electrode which was also verified by comparing

electrochemical impedance spectroscopy of NVTO/ITO electrode, TiO_2/ITO electrode and ITO electrode (Figure S2). Moreover, the uniform dispersion of NVTO nanoparticles in the CHIT network promoted electron transfer due to the generation of surface oxygen vacancies. After the immobilization of probe DNA onto the electrodes, the peak current (curve d) decreased due to the immobilization of DNA, which blocked the electron transfer between electrode and the redox probes in the solution [25].

Electrochemical impedance spectroscopy (EIS) has been demonstrated to be an effective method for the study of the interfacial properties of surface-modified electrodes[26,27]. Figure 3B presented the EIS of surface-modified electrodes obtained at open circuit potential along with the equivalent circuit in the frequency range of $10^5 \sim 10^{-2}$ Hz. In EIS, the total impedance was determined by various parameters, including solution resistance (R_s), double layer capacitance (C_{dl}), charge transfer resistance (R_{ct}) and Warburg element (Z_w). The R_s and Z_w values, representing the resistance of the electrolyte solution and the diffusion of the applied redox probe, respectively, were not affected by biochemical reactions occurring on the electrode's interface. C_{dl} and R_{ct}, however, were dependent upon the dielectric and insulating features at the electrode/electrolyte interface, respectively. The semicircular portion of the EIS curve corresponds to an electron transfer-limited process and its diameter is equal to the electron transfer resistance, R_{ct}, which controlled the electron transfer kinetics of the redox probe at the electrode's interface.

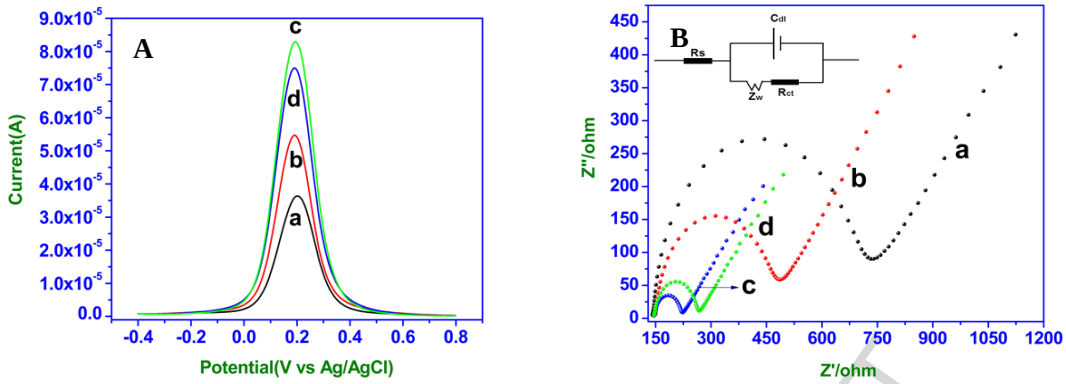

Figure 3 (A) Differential pulse voltammetry (DPV) of (a) ITO electrode, (b) CHIT/ITO electrode, (c) CHIT-NVTO/ITO electrode，(d) ssDNA/CHIT-NVTO /ITO bioelectrode, (B) Electrochemical impedance spectroscopy of the test electrodes: (a) ITO electrode, (b) CHIT/ITO electrode, (c) CHIT-NVTO/ITO electrode，(d) ssDNA/CHIT- NVTO/ITO bioelectrode.

Table 2 R_{CT} of the test electrodes

Electrodes	ITO	CHIT/ITO	CHIT-NVTO/ITO	ssDNA/CHIT-NVTO/ITO
R_{CT}（Ω）	517.2	358.6	173.4	202.5

The diameter of the semicircle (R_{ct}) was the characteristic of the diffusion limiting step of the electrochemical process. As was summarized in Table 2, we can see that the R_{ct} values of various modified electrodes are 517.2Ω (ITO), 358.6Ω (CHIT/ITO), 183.4Ω (CHIT-NVTO/ITO), and 202.5Ω (ssDNA/CHIT-NVTO/ITO), respectively. The electron transfer resistance decreased in the order: bare ITO > CHIT/ITO > ssDNA/CHIT-NVTO/ITO > CHIT-NVTO/ITO, implying easier electron transfer between the solution and the electrode in the CHIT-NVTO nanocomposite film; CHIT-NVTO nanocomposite film provide increased electroactive surface, plus promote electron transfer between the electrode and DNA. However, the DNA layer acted as a barrier for electron transfer between the electrode surface and the redox

probes in the solution[28], which confirmed the immobilization of probe DNA onto the CHIT-NVTO/ITO electrodes, presumably due to the insulating characteristics of biomolecules.

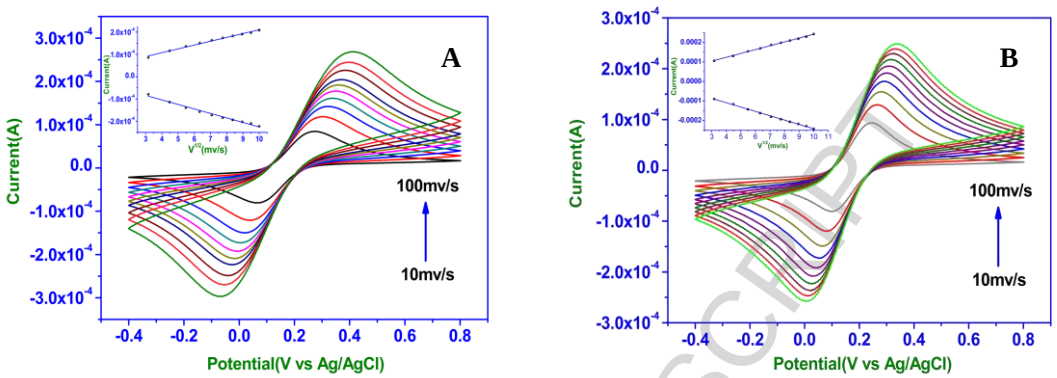

Figure 4 (A) Cyclic voltamograms of the ssDNA/CHIT/ITO bioelectrode at scan rates of 10~100mV/s, inset: magnitude of the current as a function of scan rate. (B) Cyclic voltamograms of the ssDNA/CHIT-NVTO/ITO bioelectrode at scan rates of 10~100mV/s, inset: magnitude of the current as a function of scan rate.

Figure 4 exhibited cyclic voltamograms of the ssDNA/CHIT/ITO bioelectrode and ssDNA/CHIT-NVTO/ITO bioelectrode in PBS (pH 7.0) as a function of scan rate (from 10 to 100mV/s), respectively. Two bioelectrodes' anodic (I_a) and cathodic (I_c) currents were linearly proportional to the scan rate (inset, Figure 4A and Figure 4B) according to Eq.1-1, 1-2, 2-1 and 2-1, respectively, which indicates a typical diffusion-controlled electrochemical behavior.

$$I_a(A)_{(\text{ssDNA/CHIT/ITO})} = 3.890\times10^{-5}A + 1.718\times10^{-5}A\times v^{1/2} \qquad \text{(Eq.1-1)}$$

$$I_c(A)_{(\text{ssDNA/CHIT/ITO})} = -2.328\times10^{-5}A - 2.024\times10^{-5}A\times v^{1/2} \qquad \text{(Eq.1-2)}$$

$$I_a(A)_{(\text{CHIT-NVTO/ITO})} = 4.455\times10^{-5}A + 1.975\times10^{-5}A\times v^{1/2} \qquad \text{(Eq.2-1)}$$

$$I_c(A)_{(\text{CHIT-NVTO/ITO})} = -2.018\times10^{-5}A - 2.222\times10^{-5}A\times v^{1/2} \qquad \text{(Eq.2-2)}$$

where v was scan rate (mV/s); the square of the correlation coefficient, (Eq.1-1)R^2 = 0.991, (Eq.1-2) R^2 = 0.987, (Eq. 2-1) R^2 = 0.998 and (Eq. 2-2) R^2 = 0.998.

The surface concentration of the GOx/CHIT–NVTO/ITO bioelectrode has been estimated using Eq. 3:

$$I_p = 0.227nFAC^*_0 \times k^0 \exp\left[\frac{-\alpha n_a F}{RT}(E_p - E^{\theta'})\right] \quad \text{(Eq.3)}$$

where I_p was the anodic peak current, n was the number of electrons transferred (1), F was the Faraday constant (96485.34 $C \cdot mol^{-1}$), A was the surface area (0.25 cm^2), R was the gas constant (8.314 $J \cdot mol^{-1} \cdot K^{-1}$), C^*_0 was the surface concentration of ionic species on the film surface ($mol \cdot cm^{-2}$), E_p was the peak potential and $E^{\theta'}$ was the formal potential. ($-\alpha n_a F/RT$) and k_0 (rate constant) correspond to the slope and intercept of the $\ln(I_p)$ *vs* E_p-$E^{\theta'}$ curve at different scan rates. The ssDNA/CHIT-NVTO/ITO bioelectrode increased the surface concentration by an estimated as 4.9×10^{-6} $mol \cdot cm^{-2}$ that was higher than ssDNA/CHIT/ITO bioelectrode's surface concentration (2.8×10^{-6} $mol \cdot cm^{-2}$), indicating that the NVTO nanoparticles can increase electroactive surface area of bioelectrode.

3.4 Performance of the DNA biosensor

The selectivity of this electrochemical DNA biosensor was investigated by using the ssDNA/CHIT-NVTO/ITO bioelectrode to hybridize with different target ssDNA (one mismatches, two-base mismatches and noncomplementary) sequences. After hybridization of the DNA probe, the changes of the Nyquist diagram are shown in Figure 5. The curve a was the Nyquist diagram at the probe ssDNA/ CHIT-NVTO/ITO bioelectrode. After hybridization of the DNA probe with cDNA,

the change of the Nyquist diagram is shown in curve b. The R_{ct} value increased obviously, suggesting that hybrids (dsDNA) were formed at the electrode. After the DNA probe was hybridized with the single-base mismatched sequence (curve c and curve d) or double-base mismatched sequence (curve e and curve f), the increase of the R_{ct} value was much smaller than that obtained from the hybridization with cDNA (curve b). And the single-base mismatched sequence and double-base mismatched sequence could also be recognized via comparing the increase of the R_{ct} value. The increase of the R_{ct} value was negligible after the DNA probe was hybridized with the noncomplementary sequence (curve g), indicating that the hybridization reaction was not achieved. The results demonstrated that this DNA biosensor displayed very high selectivity for the hybridization detection.

In this paper, the reproductibility of the biosensor was monitored by eight parallel-made DNA biosensors to detect 1.0×10^{-10} M target DNA (Figure 5B), and the results showed that a relative standard deviation (RSD) of 1.01% (n=8) was estimated, showing a high reproductibility of the constructed DNA biosensor. The stability of the modified electrode was further investigated. Store of ssDNA/ CHIT-NVTO/ITO at 4℃ for 60 days resulted in a change of 9.6% in the initial R_{ct} response; In addition, the R_{ct} response was no change after the modified electrode immersed in the 20 mL TE buffer solution for 10h, indicating this modified electrode was a stable platform for ssDNA probe immobilization.

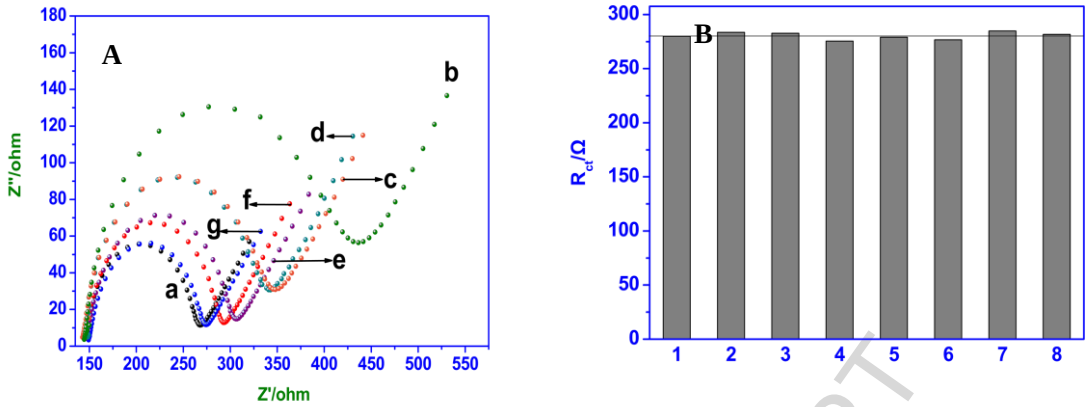

Figure 5 (A) Electrochemical impedance spectroscopy of the test electrodes: (a) ssDNA/CHIT-NVTO/ITO bioelectrode, (b) dsDNA/CHIT-NVTO/ITO bioelectrode, (c) OBM1/CHIT-NVTO /ITO bioelectrode, (d) OBM2/CHIT-NVTO/ITO bioelectrode, (e) TBM1/CHIT-NVTO/ITO bioelectrode, (f) TBM2/CHIT-NVTO/ITO bioelectrode, (g) ncDNA/CHIT-NVTO/ITO bioelectrode. (B) Reproducibility of ssDNA/ CHIT-NVTO/ITO bioelectrode.

Figure 6 shows the results of response studies carried out with respect to the different concentration of target DNA sequence with ssDNA/ CHIT-NVTO/ITO bioelectrode using EIS in PBS (50mM, pH 7.0, 0.9%NaCl) containing 1mM $[Fe(CN)_6]^{3-/4-}$. The dynamic detection range for the sequence-specific DNA in the hybridization solution was changed from 1.0×10^{-15} M to 1.0×10^{-6} M. As showed in Figure 6B, the R_{ct} values showed a gradual increase with the increase of target DNA concentrations in the hybridization solution. The difference values (ΔR_{ct}) between before and after hybridization were found to be well proportional to the logarithm of target DNA concentration in the range from 1.0×10^{-15} M to 1.0×10^{-6} M. The linear regression equation was ΔR_{ct} = 220.8927+14.6879 log C (C was the concentration of target DNA) with a regression coefficient R=0.9973. The detection limit was 1.09×10^{-16} M (S/N=3). The results demonstrated that the sensitivity of this

impedimetric DNA biosensor was good enough for the BRCA1 gene sequence detection.

The performance of the proposed biosensor was compared with reported DNA electrochemical biosensors and listed in Table 3. It is apparent that the proposed DNA biosensor had a much wider detection range and lower detection limit for the target DNA assay.

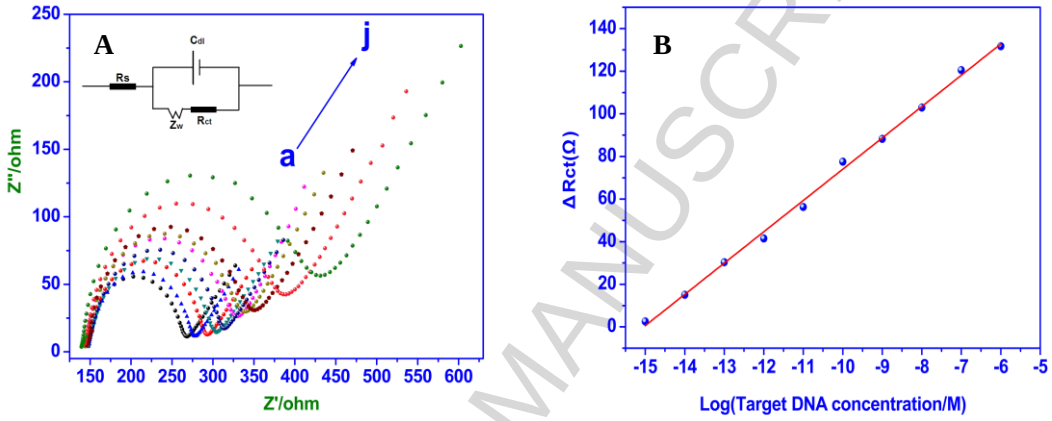

Figure 6 (A) Electrochemical impedance spectroscopy of ssDNA/CHIT-NVTO/ITO bioelectrode after hybridization reaction with different concentrations of sequence-specific DNA of BRCA1 gene: (a) 1.0×10^{-15} mol/L,(b) 1.0×10^{-14} mol/L, (c) 1.0×10^{-13} mol/L, (d) 1.0×10^{-12} mol/L, (e)1.0×10^{-11}mol/L, (f) 1.0×10^{-10} mol/L, (g) 1.0×10^{-9} mol/L, (h) 1.0×10^{-8} mol/L, (i) 1.0×10^{-7} mol/L and (j) 1.0×10^{-6} mol/L. (B) Plot of ΔRct *vs* logarithm of target DNA concentration

Table 3 Comparison of the performance of the proposed biosensor with other modified electrodes.

Electrodes	Detection method	Linear range (mol/L)	Limit of Detection (mol/L)	References
CS–MWNTs/GCE	EIS	1.0×10^{-11} ~1.0×10^{-6}	8.5×10^{-14}	[24]
HGN/Au	DPV	1×10^{-12} ~1×10^{-8}	1×10^{-12}	[25]
MWNTs/ZrO_2 /GCE	DPV	1.49×10^{-10}~9.32×10^{-8}	7.5×10^{-11}	[26]
CHIT-NVTO/ITO	EIS	1.0×10^{-15}~1.0×10^{-6}	1.09×10^{-15}	Present work

4. Conclusions

In this paper, a high-efficiency electrochemical DNA biosensor based on a novel CHIT-NVTO thin film was developed for detection of BRCA1 from breast cancers gene. The synergistic effects of both NVTO nanoparticles and chitosan anchored on the electrode surface magnified the electrochemical response due to their large surface area and excellent electronic conductivity, which improved the sensitivity of the proposed biosensor. The electrochemical DNA biosensor was applied to the detection of BRCA1 gene sequence with a dynamic concentration range from 1.0×10^{-15} to 1.0×10^{-6} M and a low detection limit of 1.09×10^{-16} M (S/N=3). These results indicated that the biosensor showed the advantages such as simple preparation procedure, high selectivity, low cost, high sensitivity, fast response and wide dynamic detection range. The remarkable electrochemical properties of the CHIT-NVTO composite may offer new approach for developing novel types of highly sensitive and stable electrochemical biosensor.

Acknowledgement

All the authors thank the Science and Technology Planning Project of Guangzhou (No. 2009Z2-D511) China, for financial support.

References

1 A. Tiwaria, S.Q. Gong, Electrochemical detection of a breast cancer susceptible gene using cDNAimmobilized chitosan- co-polyaniline electrode, Talanta 77(2009) 1217-1222.

2 M. Kasumi, Study suggests blood test can accurately detect breast cancer, Bioanalysis 6 (2014) 433-435.

3 P. Economopoulou, G. Dimitriadis, A. Psyrri, Beyond BRCA: New hereditary breast cancer susceptibility genes, Cancer Treatment Reviews 4 (2015) 1-8.

4 U.M. Jhanwar, BRCA1 in cancer, cell cycle and genomic stability, Frontiers in Bioscience 8 (2003) 1107-1117.

5 M. Culha, D. Stokes, L.R. Allain, T.V. Dinh, Surface-enhanced Raman scattering substrate

based on a self-assembled monolayer for use in gene diagnostics, Analytical Chemistry 75 (2003) 6196-6201.

6 L.H. Castilla, F.J. Couch, M.R. Erdos, K.F. Hoskins, K. Calzone, J.E. Garber, J. Boyd, M.B. Lubin, M.L. Deshano, L.C. Brody, F.S. Collins, B.L. Weber, Mutations in the BRCA1 gene in families with early-onset breast and ovarian cancer, Nature Genetics 8(1994) 387-391.

7 J.F. Thompson, J.G. Reifenberger, E. Giladi, K. Kerouac, J. Gill, E. Hansen, A. Kahvejian, P. Kapranov, T. Knope, D. Lipson, K.E. Steinmann, P.M. Milos, Single-step capture and sequencing of natural DNA for detection of BRCA1 mutations, Genome Research 22 (2012) 340-345.

8 G.U. Flechsig, T. Reske, Electrochemical detection of DNA hybridization by means of osmium tetroxide complexes and protective oligonucleotides, Analytical Chemistry 79 (2007) 2125-2130.

9 X.M. Li, J.P. Xia, S.S. Zhang, Label-free detection of DNA hybridization based on poly(indole-5-carboxylic acid) conducting polymer, Analytica Chimica Acta 622 (2008) 104-110.

10 Z.H. Wang, N. Sun, Y. He, Y. Liu, J.H. Li, DNA assembled gold nanoparticles polymeric network blocks modular highly sensitive electrochemical biosensors for protein kinase activity analysis and inhibition, Analytical Chemistry 86 (2014) 6153-6159.

11 C.Y. Yang , B.T. Dou, K. Shi, Y.Q. Chai, Y. Xiang, R. Yuan, Multiplexed and amplified electronic sensor for the detection of microRNAs from cancer cells. Analytical Chemistry 86 (2014) 11913-11918.

12 F.F. Deng, C. Ding, Y. Wang, W.T. Li, L.L. Liu, H. Li, A shell-like Sm-doped CeO_2 nanostructure based electrochemical DNA biosensor for breast cancer gene sequence detection, Analytical methods 6 (2014) 9228-9233.

13 R. Singh, R. Verma, A. Kaushik, G. Sumana, S. Sood, R.K. Gupta, B.D. Malhotra, Chitosan–iron oxide nano-composite platform for mismatch-discriminating DNA hybridization for Neisseria gonorrhoeae detection causing sexually transmitted disease, Biosensors and Bioelectronics 26 (2011) 2967-2974.

14 W. Sun, P. Qin, H.W. Gao, G.C. Li, K. Jiao, Electrochemical DNA biosensor based on chitosan/ nano-V_2O_5/MWCNTs composite film modified carbon ionic liquid electrode and its application to the LAMP product of Yersinia enterocolitica gene sequence, Biosensors and Bioelectronics 25 (2010) 1264-1270.

15 N. Zhang, K. Zhang, L. Zhang, H.Y. Wang, H.W. Shi, C. Wang, A label-free electrochemical DNA sensor based on ZrO_2/poly(thionine)/CNT modified electrode and its application for detecting CaMV35S transgene gene sequence, Analytical methods 7 (2015) 3164-3168.

16 R. Imani, A. Iglic, A.P.F. Turner, A. Tiwari, Electrochemical detection of DNA damage through visible-light-induced ROS using mesoporous TiO_2 microbeads, Electrochemistry Communications 40 (2014) 84-87.

17 N.A. Peppas, J.Z. Hilt, A. Khademhosseini, R. Langer, Hydrogels in biology and medicine: from molecular principles to bionanotechnology, Advanced Materials 18 (2006) 1345-1360.

18 C. Peniche, W. Argüelles-Monal, N. Davidenko, R. Sastre, A. Gallardo, J.S. Román, Self-curing membranes of chitosan/PAA IPNs obtained by radical polymerization: preparation, character- ization and interpolymer complexation, Biomaterials 20 (1999) 1869-1878.

19 X.L. Luo, J.J. Xu, J.L. Wang, H.Y. Chen, Electrochemically deposited nano-composite of chitosan and carbon nanotubes for biosensor application, Chemical Communications 16 (2005) 2169-2171.

20 H.L. Fan, L.L. Wang, K.K. Zhao, N. Li, Z.J. Shi, Z.G. Ge, Z.X. Jin, Fabrication, Mechanical properties, and biocompatibility of graphene-reinforced chitosan composites, Biomacromolecules 11 (2010) 2345-2351.

21 N.R. Elezović, B.M. Babić, L.G. Krstajić, V. Radmilović, N.V. Krstajić, L.J. Vračar, Synthesis, characterization and electrocatalytical behavior of Nb–TiO_2/Pt nanocatalyst for oxygen reduction reaction, J. Power Sources 195(2010) 3961-3968.

22 K. Karthik, S.K. Pandian, N.V. Jaya, Effect of nickel doping on structural, optical and electrical properties of TiO_2 nanoparticles by sol–gel method, Applied Surface Science 256 (2010) 6829-6833.

23 H. Li, X.W. Huang, J.L. Lu, F. Sun, F.Y. Yi, Y. Wang, Y.W. Tang, A novel glucose biosensor fabricated with electroactive Nb0.95Ti0.95O4 nano-composite film, Int. J. Electrochem. Sci., 7 (2012) 9354 – 9365.

24 J. Li, L.T. Piehler, D. Qin, J.R. Baker, D.A. Tomalia, D.J. Meier, Visualization and characterization of poly(amidoamine) dendrimers by atomic force microscopy, Langmuir 16 (2000) 5613-5616.

25 Y.Y. Qiu, H.Fan, X. Liu, S.Y. Ai,T.T. Tang, R.X.Han, Electrochemical detection of DNA damage induced by in situ generated bisphenol A radicals through electro-oxidation, Microchimica Acta 171(2010)363-369.

26 P.Yadav, K.Pandey, P.Bhatt, B.Tripathi, M.K.Pandey, M.Kumar, Probing the electrochemical properties of TiO_2/graphene composite by cyclic voltammetry and impedance spectroscopy, Materials Science and Engineering: B 206(2016)22-29.

27 J.Tymoczko, V.Colic, A.S. Bandarenka, W.Schuhmann, Detection of 2D phase transitions at the electrode/electrolyte interface using electrochemical impedance spectroscopy, Surface Science 631(2015)81-87.

28 A.Rabtia,N.Raouafib, A.Merkoçi, Bio(Sensing) devices based on ferrocene-functionalized graphene and carbon nanotubes, Carbon, 108(2016)481-514.

Highlights

1. **A novel (Nb,V) codoped TiO_2 was synthesized.**
2. **A novel sensitive impedimetric DNA biosensor was fabricated.**
3. **The proposed biosensor owned high sensitivity, wide linear range and low detection limit.**